Metallography, Microstructure, and Analysis (2021) 10:441–447
https://doi.org/10.1007/s13632-021-00760-8

TECHNICAL ARTICLE

The Effect of Time and Temperature of Solutionizing Heat Treatment on γ′ Characterization in a Ni-Base Superalloy

Yazdan Shajari[1] · Seyed Hossein Razavi[2] · Zahra Sadat Seyedraoufi[3] · Mohsen Samiee[3]

Received: 16 February 2021 / Revised: 15 July 2021 / Accepted: 19 July 2021 / Published online: 11 August 2021

Abstract

Nickel-base superalloys are being used widely in the air and land-based gas turbines. The primary strengthening mechanism of these alloys is the distribution of the γ′(Ni_3 (Al, Ti)) intermetallic phase. This phase is formed in two stages, including the solutionizing and aging heat treatments. In order to create a structure with the desirable properties, the solutionizing heat treatment is more important than aging. In this research, solutionizing heat treatment was conducted at different temperatures and times, and aging heat treatment was carried out at a constant temperature of 850°C for 24 h. γ′ precipitates characterization was done by scanning electron microscopy and field emission scanning electron microscopy. The results showed that the volume fraction and size of secondary γ′ precipitates decreases as the temperature and time of the solutionizing heat treatment increases. Therefore, after the aging, size and volume fraction of γ′ precipitates initially increased and then decreased.

Keywords Nickel-base superalloys · γ′ Precipitates · Solutionizing treatment · Characterization

Introduction

Superalloys are advanced and strategic materials that can maintain their engineering properties at temperatures above their recrystallization temperature. Some of these alloys are strengthened by the formation and distribution of coherent γ′ (Ni3(Al, Ti)) precipitates, which prevent the movement of dislocations via anti-phase boundaries [1, 2]. The microstructure and mechanical behavior of Ni-base superalloy depends on the primary and secondary production processes (solutionizing and aging). Hence, the heat treatment of these alloys plays a significant role in their mechanical properties (both at room temperature and at high temperatures) [3].

Secondary production processes such as heat treatment, welding, and coating are applied on Ni-base superalloys to improve their quality. The heat treatment of these alloys has two main steps including solutionizing and aging, which depends on the desired properties and number of each step that determined [4].

According to the phase diagram, through the placement of alloy at a temperature of a single-phase region with sufficient time, a single-phase or multiphase alloy with a low percentage of secondary phases will form. Afterward, the alloy is aged for a long time by placing it in the two-phase zone. The supersaturated matrix in the solutionizing step is a facilitator for nucleation and growth of γ′ precipitates during the aging. Therefore, the higher quality solutionizing increases the volume fraction of secondary γ′ after aging [5].

The change in the Gibbs free energy due to γ′ precipitation is obtainable from the below equation:

$$\Delta G = -V\Delta G_{\mathrm{V}} + A_{\gamma} + V\Delta G_{\mathrm{S}} \quad (1)$$

where γ is the interface energy of precipitate per unit area, A is surface of a new interface and matrix, ΔG_{V} is free energy resulted from the formation of a precipitate and ΔG_{S} is strain energy. The interaction between free chemical energy and energy of interface is effective for nucleation of γ′ precipitates. as a result, as the amount of solid supersaturated solution increases, the free chemical energy increases, and consequently, the size of the critical nucleus will reduce [6–8].

The nucleation rate of γ′ precipitates during the aging process depends on the amount of supersaturation created in the solutionizing heat treatment. Also, an appropriate structure

✉ Zahra Sadat Seyedraoufi
z.seyedraoufi@kiau.ac.ir

[1] Materials and Energy Research Center, 14155-4777 Karaj, Iran

[2] School of Metallurgy and Materials Engineering, Iran University of Science and Technology (IUST), Tehran, Iran

[3] Department of Materials Engineering, Karaj Branch, Islamic Azad University, Karaj, Iran

after the aging is highly contingent on the proper solutionizing heat treatment [9].

The solutionizing heat treatment of Ni-Base superalloys depends on the diffusion parameters, which is an equilibrium process between the solutionizing and precipitation. On the one side of this equilibrium is the dissolution of small and large γ precipitates, and on the other side of this equilibrium is γ' agglomeration and precipitation [10, 11].

The aim of this study is choose of the most suitable solutionizing condition for Ni-base superalloy along with investigating the effect of solutionizing parameters on microstructure, especially nano γ' precipitates.

Experimental Method

In this study, a part of the worked IN738LC in the riser of a gas turbine blade was used. According to Fig. 1, cylindrical samples were prepared in 10 mm diameter and 10 mm length by electrical discharge machining. Table 1 shows the chemical composition of the used superalloy by weight percentage. Furthermore, the sample was heat-treated in a tubular furnace under the protection of the argon gas. The solutionizing heat treatment was carried out in a temperature range of 1090–1200 °C at different times. After, the aging was done in constant temperature at 850 °C for 24 h. The schematic image of various solutionizing conditions along with stable conditions of aging has been shown in Fig. 2. Also, the various conditions of heat treatment are brought up in Table 2. Immediately after solutionizing and aging, the microhardness of the samples was measured, according to ASTM E82-16 under the load of 100 g for 15 s [12]. After each step of heat treatment, the microstructural studies were performed. After preparing, grinding, and polishing, samples were electro-etched by 170 ml H_3PO_4, 10 ml H_2SO_4 and 16 mg CrO_3 under the potential differentiate of 4–6 V for 4 s [13]. The samples were studied by SEM (VEGA/TESCAN) after the solutionizing treatment and FESEM (MIRA3 made by the Czech Republic) after the aging.

Results and Discussion

The OM image of the as-casted alloy is shown in Fig. 3. As is clear, significant quantities of γ' precipitates are observable in the form of stretched and compact masses. Large amount of carbide with a size of about 13 µm indicates the proper time of solidification and growth of MC carbide blocks. The phase that firstly solidifies is MC carbide blocks that formed in the melt. Moreover, since this phase

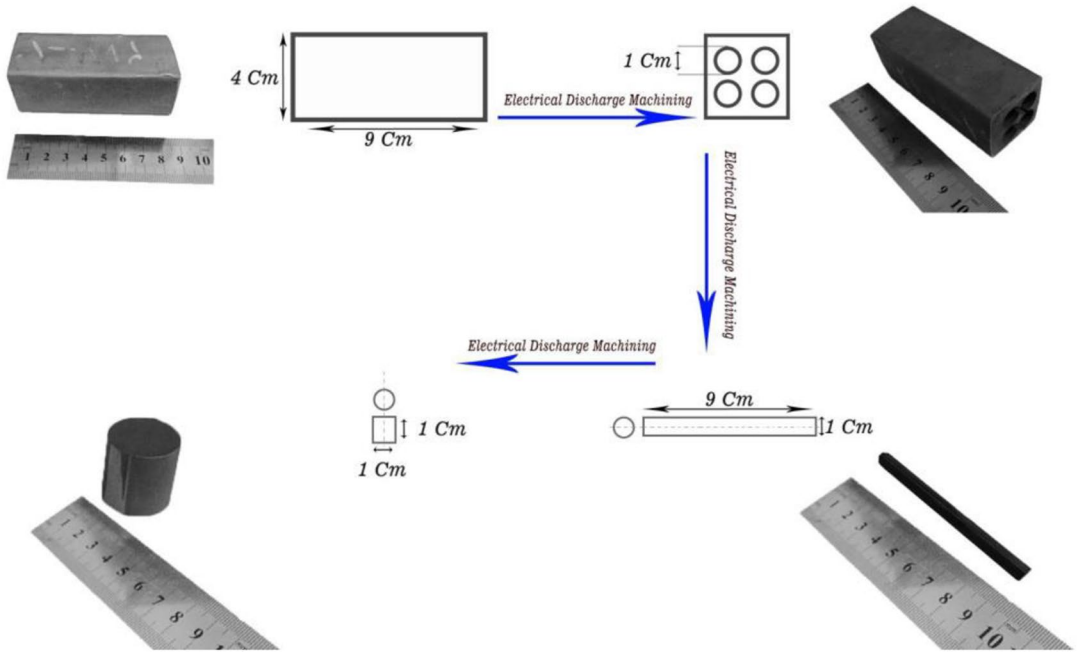

Fig. 1 Sample preparation steps

Table 1 Chemical composition of the used IN738LC (wt.%)

Element	C	Cr	Mo	Co	Ni	Ta	W	Al	Ti	Zr	B	Fe
wt.%	0.11	16.01	1.80	8.31	Base	2.01	3.00	3.40	3.23	0.05	0.01	0.15

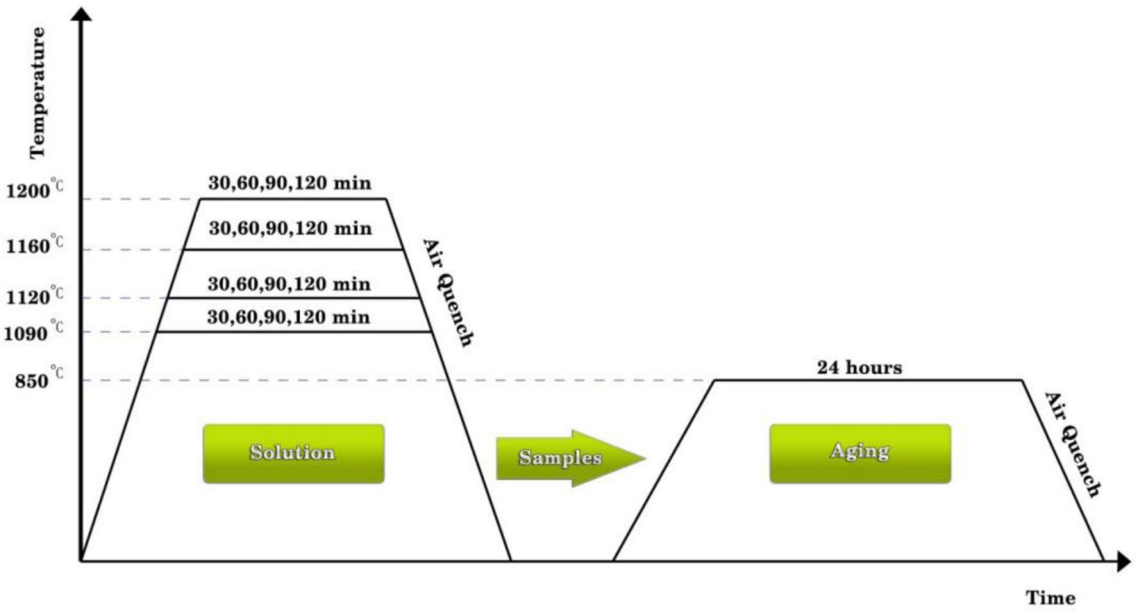

Fig. 2 Schematic of the heat treatment cycle

Table 2 The heat treatment conditions

Samples	Solution	Aging
RF1	1090 °C–30 min	850 °C–24 h
RF2	1090 °C–60 min	850 °C–24 h
RF3	1090 °C–90 min	850 °C–24 h
RF4	1090 °C–120 min	850 °C–24 h
RF5	1120 °C–30 min	850 °C–24 h
RF6	1120 °C–60 min	850 °C–24 h
RF7	1120 °C–90 min	850 °C–24 h
RF8	1120 °C–120 min	850 °C–24 h
RF9	1160 °C–30 min	850 °C–24 h
RF10	1160 °C–60 min	850 °C–24 h
RF11	1160 °C–90 min	850 °C–24 h
RF12	1160 °C–120 min	850 °C–24 h
RF13	1200 °C–30 min	850 °C–24 h
RF14	1200 °C–60 min	850 °C–24 h
RF15	1200 °C–90 min	850 °C–24 h
RF16	1200 °C–120 min	850 °C–24 h

is suspended in the melt, it can be observed in any form in the γ matrix [14].

In Fig. 4a, the SEM image shows the solution heat-treated sample at 1090 °C for 30 min. As can be seen, the γ–γ' eutectic phase is about to dissolve, which is the first phase to solutionize in the IN738LC superalloy [15]. The SEM image, Fig. 4b, shows the sample that solution heat-treated at 1090 °C for 120 min. This image illustrates that as the time of solutionizing increases at constant temperature, a suitable condition for agglomeration of γ' precipitates will

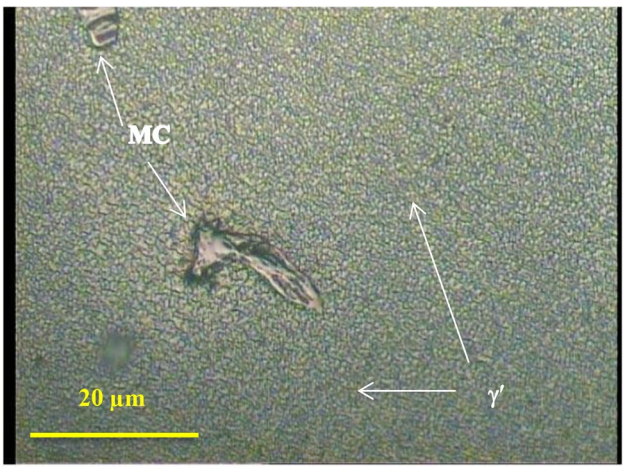

Fig. 3 OM image of as casted sample

be provided. In Fig. 4c, the SEM image depicts the sample, which solutionized at 1200 °C for 120 min. In visual comparative, by increasing the temperature of solutionizing heat treatment, the volume fraction of γ' decreases. Quantitative information of residual precipitates is shown in Table 3. Figure 3 and Table 3 demonstrate that volume fraction and size of γ' precipitates decrease as the time and temperature of solutionizing heat treatment increase. After solutionizing, according to evidence and current mechanisms, γ' precipitates can be classified as follows:

a. Large γ' precipitates formed by the agglomeration of other precipitates.

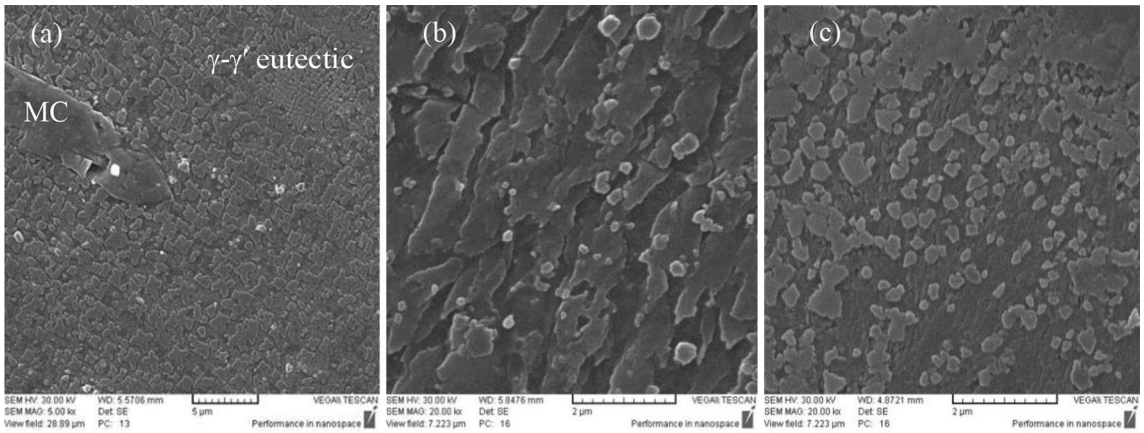

Fig. 4 SEM images of solutionized samples: (**a**) RF1, (**b**) RF4, (**c**) RF16

Table 3 Characteristics of γ' precipitates after solutionizing heat treatment

Samples	Total volume fraction of γ' (%)	Volume fraction of nano γ' (%)	Volume FRACTION of big γ' (%)	Size of small γ' (μm)	Size of large γ' (μm)
As casted	87.64	…	…	0.095	2.03
RF1	76.44	23.06	53.38	0.07568	1. 98
RF4	72.75	22.11	50.64	0.07142	1.90
RF16	64.97	37.77	27.77	0.05950	1.40

b. Nano or submicron precipitates, which resulted from large precipitates.
c. Nano γ′ precipitate, which nucleated during solutionizing heat treatment.
d. Nano γ′ precipitates formed during the quench, known as cooling precipitates.

Table 3 shows characteristics of γ' precipitates after solutionizing heat treatment.

Increasing the time and temperature of solutionizing heat treatment leads to a decrease in the volume fraction of precipitates of the first type while it can result in increase in the volume fraction of nano precipitates and precipitates' size. At the beginning of solutionizing heat treatment, γ′ precipitates dissolve from their corners, leading to a rise of stabilizing elements around the matrix which then becomes enriched with γ′. As time increases, precipitates join each other through diffusion in Al and Ti rich directions. Although this phenomenon causes the formation of large precipitates, these precipitates are smaller in comparison to coarse γ′ precipitates in the as-casted sample. As the supersaturation increases in the matrix, movement of the atoms toward each other becomes hard due to the formation of large precipitates and the nucleation of γ′ precipitates during solutionizing [16]. Therefore, in high temperatures, the rate of agglomeration decreases. Hence, it can be said that γ′ precipitates are affected by changes in the temperature and the time of the solutionizing heat treatment.

Figure 5a shows the SEM image of the RF1 sample after the solutionizing heat treatment. In this image, nano γ′ precipitates are well distinguishable. As mentioned before, around the coarse precipitates, nucleation of nano γ′ precipitates is more probable. Supersaturation and lack of energy brings these precipitates closer together and prompt them to grow. In Fig. 5b, the SEM image shows nano γ′ precipitates after solutionizing heat treatment in the RF16 sample where the precipitates have agglomerated; this is due to the suitability of the diffusion path and the amount of supersaturation.

Figure 6a shows the FESEM image of the RF1 sample after the aging. This image demonstrates the primary and large γ′ precipitates with an irregular shape along with secondary nano γ′ precipitates with a relatively high-volume fraction. Figure 6b demonstrates the FESEM image of the RF4 sample after the aging where the primary γ′ precipitates are in cubic shape. The FESEM image of the RF16 sample after aging is shown in Fig. 6c. In this sample, the high temperature of solutionizing heat treatment leads to a low volume fraction of precipitates, where precipitates with small size increase the number of nano precipitates and produce more secondary precipitates [6].

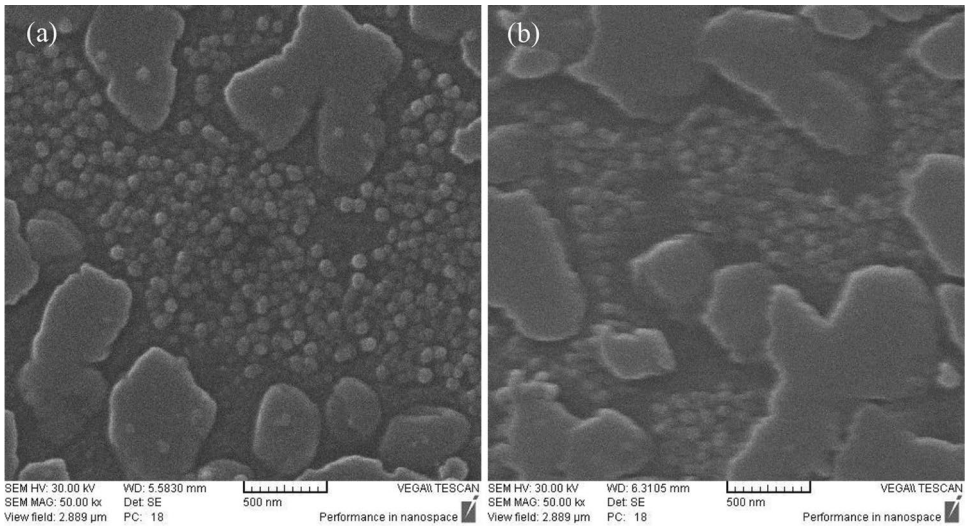

Fig. 5 SEM images of nano precipitates remained in solutionized samples: (**a**) RF1, (**b**) RF16

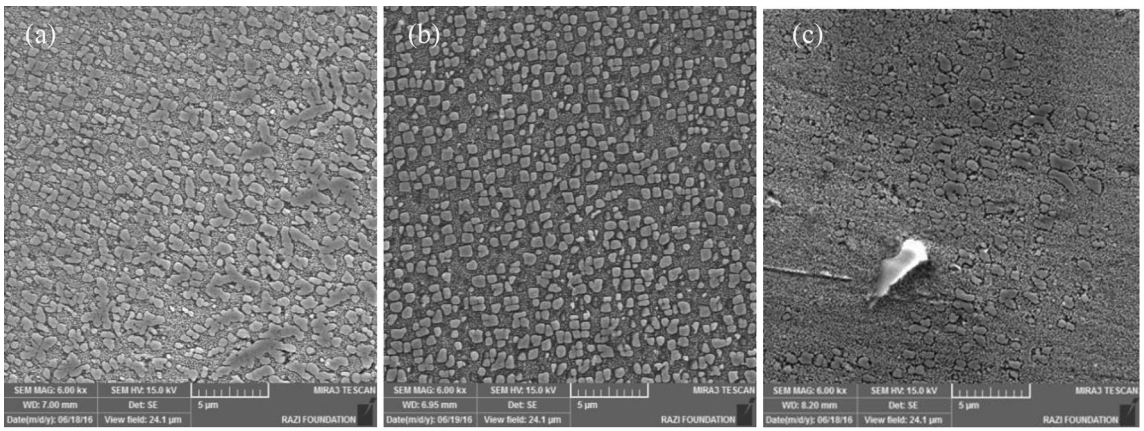

Fig. 6 FESEM images of samples after aging: (**a**) RF1, (**b**) RF4, (**c**) RF16

Primary γ' precipitates' size is visible in Fig. 6a, where the solutionizing conditions were not suitable in the RF1 sample. After the solutionizing, residual γ' precipitates grow during the aging and as the time passes secondary nano γ' precipitates agglomerate and join where eventually form large precipitates. In Fig. 6b, cubic γ' with appropriate size indicates the suitable condition of the solutionizing and the formation of a superior microstructure in comparison with the RF1 sample. Increasing the time of solutionizing heat treatment leads to an increase in the volume fraction of soluble γ' precipitates and supersaturation of the solution. Accordingly, this will create more suitable places for nucleation and growth of secondary nano γ' precipitates, which leads to the reduction in the size of primary and secondary γ'.

In Fig. 7a–c, the FESEM images show secondary nano γ' precipitates in RF1, RF4, and RF16 samples, respectively. As the time and temperature of the solutionizing stage increase, the size of secondary nano γ' precipitates reduces by increasing the nucleation areas. As a result, the number of precipitates increases. This increase leads to a decrease in the amount of Al and Ti in γ matrix. Due to the decrease in the chemical concentration of Al and Ti elements, the growth of γ' precipitates is limited [17]. Table 4 shows the size and volume fraction of γ' precipitates after the aging.

Dislocation interactions with precipitates and other defects lead to an increase in the hardness of Ni-base superalloy. Shearing of γ' precipitates by 1/2<110> dislocation forms an anti-phase boundary that removes by the passing of the second dislocation with a similar burgers vector. Thus, the size of γ' precipitates has a significant effect on the dislocation interaction and, consequently, hardness, and it must be controlled. It seems that the importance of the anti-phase boundary in the hardness of the IN738LC Ni-base superalloy is greater than the Orowan mechanism and stacking fault [2, 18–20]. If the size of these precipitates increases more than the required

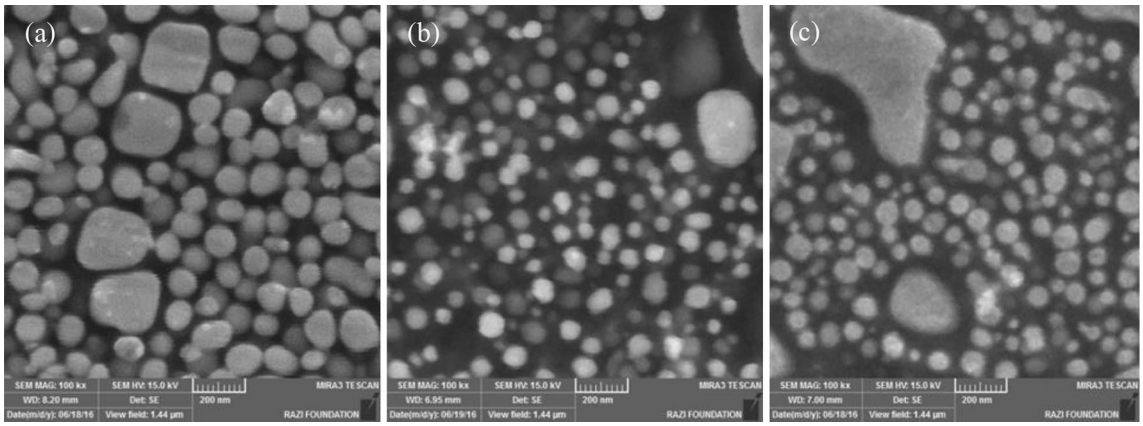

Fig. 7 FESEM images of nano secondary γ' in the aged samples: (**a**) RF1, (**b**) RF4, (**c**) RF16

Table 4 Characteristics of γ' precipitates after aging heat treatment

Samples	Total volume fraction of γ' (%)	Volume fraction of nano γ' (%)	Volume fraction of big γ' (%)	Size of small γ' (nm)	Size of large γ' (μm)
RF1	70.31	29.65	40.66	67.55	0.723
RF4	77.54	33.19	44.35	65.66	0.4912
RF16	84.16	37.95	56.21	59.22	1.1223

amount, dislocations either will cut the large precipitates by strong pairing or pass through the precipitates by the Orowan lope mechanism. Both mechanisms reduce hardness. However, if the γ' precipitates become smaller than the limited amount, they cannot be cut off, and dislocations go around them with the Orowan mechanism [21]. In solutionizing treatment, due to the decrease in size and volume fraction of γ' precipitates, the hardness reduces to half. The rate of hardness reduction increases as the time and temperature of solutionizing heat treatment increase [6, 18]. In the aging process, as the volume fraction of nano γ' precipitates increases, due to the increase in collisions between dislocations and precipitates, the hardness rises [20, 22]. In Fig. 8, the hardness changes in the samples after the solutionizing and aging heat treatments have been shown. As is clear, by increasing the time and temperature of solutionizing heat treatment, the hardness has decreased while after the aging, the hardness has increased. The formation and structural characteristics of nano γ' precipitates in both stages of precipitation-hardening according to the stated mechanisms are effective in changing the hardness.

Conclusion

The results of this study showed that time and temperature of the solutionizing heat treatment play a crucial role in the microstructure and mechanical properties of IN738LC superalloy. According to the results, increasing the temperature is more effective than increasing the time in the solutionizing stage. Besides, the increase in these parameters leads to a reduction in the size and volume fraction of γ' precipitates. In constant time, as the solutionizing temperature increases to 1200 °C, the volume fraction of γ' precipitates reduces. This reduction results in an increase in supersaturation in the gamma matrix, which is very useful in the aging stage. The γ' precipitates can be divided into four categories according to their characteristics: Large γ' precipitates formed by addition and agglomeration of other precipitates, nano or submicron precipitates which appeared from large precipitates, nano γ' precipitates nucleated during the solutionizing heat treatment, and nano γ' precipitates formed during the quenching which is known as cooling precipitates. Solutionizing at low temperatures and short times activates the agglomeration mechanism of γ' precipitates, while in high temperatures and long time, the formation of cooling precipitates increases. In the solutionizing stage, the hardness decreases due to the reduction in the size and volume fraction of the γ' phase. However, with increasing the supersaturation in the solutionizing stage, the size of secondary nano γ' decreased, whereas after aging, the volume fraction of nano γ' increased, which led to an increase in hardness.

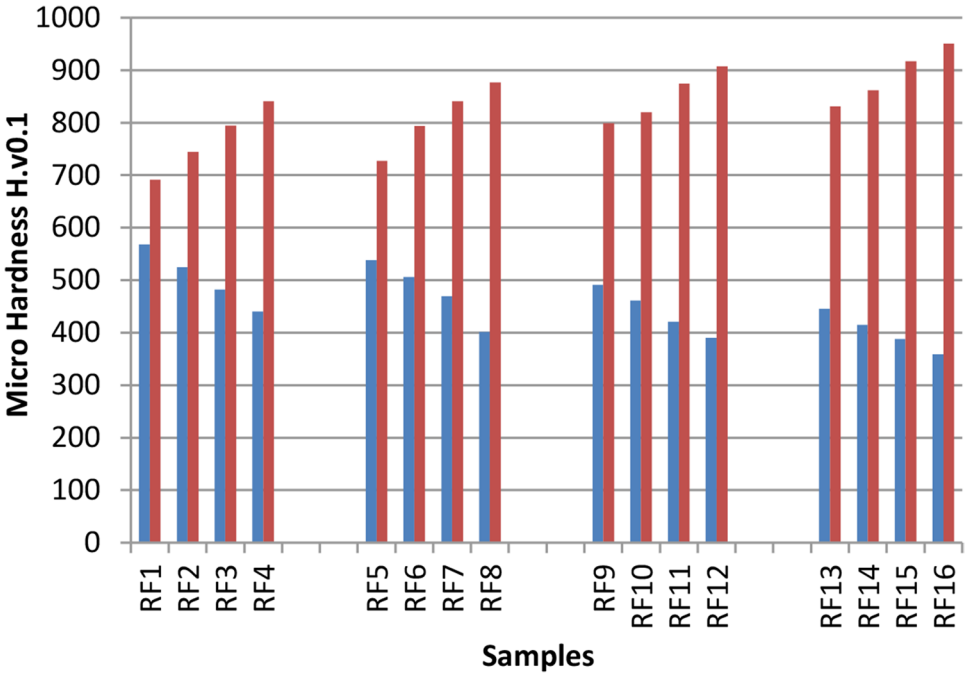

Fig. 8 Microhardness changes in samples after solutionizing and aging heat treatments under the different solutionizing conditions

References

1. A. Ges, O. Fornaro, H. Palacio, Coarsening behaviour of a Ni-base superalloy under different heat treatment conditions. Mater. Sci. Eng. A. **458**, 96–100 (2007)
2. S. Razavi, S. Mirdamadi, J. Szpunar, H. Arabi, Improvement of age-hardening process of a nickel-base superalloy IN738LC by induction aging. J. Mater. Sci. **377**, 1461–1471 (2002)
3. J. Van Sluytman, T. Pollock, Optimal precipitate shapes in nickel-base γ–γ′ alloys. Acta Mater. **604**, 1771–1783 (2012)
4. H.M. Tawancy, D.L. Klarstrom, M.F. Rothman, Development of a new nickel-base superalloy. JOM. **369**, 58–62 (1984)
5. N. El-Bagoury, M. Waly, A. Nofal, Effect of various heat treatment conditions on microstructure of cast polycrystalline IN738LC alloy. Mater. Sci. Eng. A. **487**, 152–161 (2008)
6. S.A. Sajjadi, H. Elahifar, H. Farhangi, Effects of cooling rate on the microstructure and mechanical properties of the Ni-base superalloy UDIMET 500. J. Alloys Compd. **455**, 215–220 (2008)
7. A. Singh, S. Nag, S. Chattopadhyay, Y. Ren, J. Tiley, G. Viswanathan, Mechanisms related to different generations of γ′ precipitation during continuous cooling of a nickel base superalloy. Acta. Mater. **61**, 280–293 (2013)
8. R.E. Smallman, A. Ngan, *Physical Metallurgy and Advanced Materials* (Elsevier, New York, 2011)
9. P. Sarosi, G. Viswanathan, D. Whitis, M. Mills, Imaging and characterization of fine γ′ precipitates in a commercial nickel-base superalloy. Ultramicroscopy. **103**, 83–93 (2005)
10. S.S. Hosseini, S. Nategh, A.A. Ekrami, Microstructural evolution in damaged IN738LC alloy during various steps of rejuvenation heat treatments. J. Alloys Compd. **512**, 340–350 (2012)
11. M. Ramsperger, L. Mújica Roncery, I. Lopez-Galilea, R.F. Singer, W. Theisen, C. Körner, Solution heat treatment of the single crystal nickel-base superalloy CMSX-4 fabricated by selective electron beam melting. Adv. Eng. Mater. **17**, 1486–1493 (2015)
12. E92-16 A. Standard test methods for vickers hardness and knoop hardness of metallic materials. West Conshohocken, PA. 2016.
13. A. Khodabakhshi, A. Mashreghi, Y. Shajari, S.H. Razavi, Investigation of microstructure properties and quantitative metallography by different etchants in the service-exposed nickel-based superalloy turbine blade. Trans. Indian Inst. Met. **71**, 849–859 (2018)
14. J. Yang, Q. Zheng, M. Ji, X. Sun, Z. Hu, Effects of different C contents on the microstructure, tensile properties and stress-rupture properties of IN792 alloy. Mater. Sci. Eng. A. **528**, 1534–1539 (2011)
15. E. Balikci, A. Raman, R. Mirshams, Influence of various heat treatments on the microstructure of polycrystalline IN738LC. Metall. Mater. Trans. A. **28**, 1993–2003 (1997)
16. P. Zhang, Q. Zhu, G. Chen, H. Qin, C. Wang, Effect of heat treatment process on microstructure and fatigue behavior of a nickel-base superalloy. Materials. **8**, 6179–6194 (2015)
17. R. Mitchell, M. Preuss, S. Tin, M. Hardy, The influence of cooling rate from temperatures above the γ′ solvus on morphology, mismatch and hardness in advanced polycrystalline nickel-base superalloys. Mater. Sci. Eng. A. **473**, 158–165 (2008)
18. S. Razavi, S. Mirdamadi, H. Arabi, J. Szpunar, An improved method for age hardening of a superalloy. US Provisional patent (60/309) (2001)
19. P. Wangyao, V. Krongtong, P. Tuengsook, W. Hormkrajai, N. Panich, The relationship between reheat-treatment and hardness behaviour of cast nickel superalloy GTD-111. J. Met. Mater. Miner. **16**, 2630–3508 (2006)
20. H.S. Yun, J.S. Park, S.U. An, J.M. Kim, Effect of heat treatment on the microstructural characteristics of IN738 turbine blade. Mater. Sci. Forum. Trans. Tech. Publ. **695**, 405–408 (2011)
21. D. Porter, K. Easterling, *Phase Transformations in Metals and Alloys*, 2nd edn (Chapman and Hall, New York, 1992)
22. Z. Yao, C.C. Degnan, M.A. Jepson, R.C. Thomson, Microstructural and chemical rejuvenation of a Ni-based superalloy. Metall. Mater. Trans. A. **47**, 6330–6338 (2016)